

The validation of molecular interaction among dimer chitosan with urea and creatinine using density functional theory: In application for hemodialysis membrane

by Parsaoran Siahaan

Submission date: 11-Jan-2022 03:19PM (UTC+0700)

Submission ID: 1740008416

File name: Artikel-02_Syarat_Khusus.pdf (1.88M)

Word count: 9945

Character count: 51972



The validation of molecular interaction among dimer chitosan with urea and creatinine using density functional theory: In application for hemodialysis membrane

Parsaoran Siahaan^{a,*}, Nurwarrohman Andre Sasongko^a, Retno Ariadi Lusiana^a, Vivitri Dewi Prasasty^b, Muhamad Abdulkadir Martoprawiro^c

^a Department of Chemistry, Faculty Science and Mathematics, Diponegoro University, 50275 Semarang, Indonesia

^b Faculty of Biotechnology, Atma Jaya Catholic University of Indonesia, 12930 Jakarta, Indonesia

^c Department of Chemistry, Faculty of Mathematics and Natural Sciences, Bandung Institute of Technology, 40132 Bandung, Indonesia

3

ARTICLE INFO

Article history:

Received 5 April 2020

Received in revised form 16 November 2020

Accepted 6 December 2020

Available online 10 December 2020

Keywords:

Creatinine
Chitosan
Hemodialysis
Membrane
Urea

ABSTRACT

The formation of chitosan dimer and its interaction with urea and creatinine have been investigated at the density functional theory (DFT) level (B3LYP-D3/6-31+ +G**) to study the transport phenomena in hemodialysis membrane. The interaction energy of chitosan-creatinine and chitosan-urea complexes are in range -4 kcal/mol $<$ interaction energy < -20 kcal/mol which were classified in medium hydrogen bond interaction. The chemical reactivity parameter proved that creatinine was more electrophilic and easier to bind chitosan than urea. The energy gap of HOMO-LUMO of chitosan-creatinine complex was lower than chitosan-urea complex that indicating chitosan-creatinine complex was more reactive and easier to transport electron than chitosan-urea complex. Moreover, the natural bond orbital (NBO) analysis showed a high contribution of hydrogen bond between chitosan-creatinine and chitosan-urea. The chitosan-creatinine interaction has a stronger hydrogen bond than chitosan-urea through the interaction O18-H34...N56 with stabilizing energy = -13 kcal/mol. The quantum theory atom in molecule (QTAIM) also supported NBO data. All data presented that creatinine can make hydrogen bond interaction stronger with chitosan than urea, that indicated creatinine easier to transport in the chitosan membrane than urea during hemodialysis process.

© 2020 Elsevier B.V. All rights reserved.

1. Introduction

Kidney is the largest multifunctional internal organ in the body. According to the World Health Organization (WHO), chronic kidney disease has caused the death on 5–10 million people annually [1]. One solution to overcome kidney diseases chronic is hemodialysis. Hemodialysis is a medical process to remove remaining toxic metabolite compounds from the blood patients with chronic kidney diseases. The main components of hemodialysis are a semi-permeable membrane which is allowing selective transport of toxic compounds with low molecular weight such as urea and creatinine in the blood [2,3]. Hemodialysis membranes should be biocompatible with the blood, capable to transport metabolic compounds of the blood system, selective, and non-toxic components [4,5]. Molecularly, the existence of a functional group and the formation of hydrogen bonds between the active site of the membrane active site with target molecules in the hemodialysis process are also important [6].

Normally, synthetic membranes such as polysulfone, Polyethersulfone had been used clinically as hemodialysis membranes because these polymers are easier to be manufactured [3,5]. However, the synthetic membrane has a drawback in which this type of membrane is not biodegradable, less functional group, and hydrophobic. Theoretically, Sasongko et al. (2020) had calculated the interaction between PSf with urea and creatinine using density functional theory (DFT) in which the result shows that PSf forms a weak interaction both with urea and creatinine (Toxic compounds that should be removed from the blood) [7]. Hence, many researchers try to develop hemodialysis membranes from biopolymers such as cellulose, chitosan, and others [5,8]. One of the biopolymers used for hemodialysis membrane is chitosan and its derivatives [4]. As a hemodialysis membrane, chitosan has the advantage that is purely degradable, inert, non-toxic, biocompatible, and easily modified chemically due to it has two active clusters: a cluster of amine ($-NH_2$) and hydroxyl (OH) [3–5]. Furthermore, its functional group can interact and form a hydrogen bond with creatinine or urea.

Currently, the use of theoretical approach using computational chemistry can explain the interactions that occur at the level of molecules or atoms [12–14]. Because of the advance of molecule simulation,

* Corresponding author.

E-mail address: siahaan.parsaoran@live.undip.ac.id (P. Siahaan).

3

<https://doi.org/10.1016/j.ijbiomac.2020.12.052>
0141-8130/© 2020 Elsevier B.V. All rights reserved.

computational chemistry applications have been widely used to assist many kinds of research in various fields such as health, energy, industry, environment technology, and pharmaceuticals. Costa et al. (2018) has done modeling the interaction between dimer with sodium alginate-chitosan to learn polyelectrolyte complex [12]. Deka and Bhattacharyya (2017) have calculated the dimer interaction between chitosan with essential amino acids to know and predict drug delivery effectively in the future [15]. In the case of transport phenomena in the membrane, using a theoretical approach with computational study can identify more details about the interaction between the membrane with target molecules by obtaining geometric, energetic, and electronic parameters in an appropriate molecular structure model [9,10]. Therefore, the ability of the computational approach to simulate polymer molecules is limited. Thus, chitosan is commonly calculated in the dimer structure form [7,11–14].

Studies using density functional theory dispersion correction (DFT-D3) have rekindled investigations of the nature and site of interaction between nanomaterials and biomolecules. Amidst a myriad of such studies, many computational studies are devoted to illustrating chitosan and its derivatives as gene carriers [15–17]. An equally good number of studies have shed light on different carrier molecules for protein drugs [18,19]. In this study, we focus on the interaction between chitosan-creatinine and chitosan-urea. This study aimed to evaluate the possible interactions that stabilize the chitosan-creatinine and chitosan-urea complex formation, starting from the geometry optimization of dimeric structures of chitosan, urea, and creatinine.

Moreover, a study about hydrogen bonding, HOMO LUMO energy, transfer proton, and transfer electron were also analyzed. The density functional theory (DFT-D3) and natural bond orbital (NBO) methods were employed. This study can suggest the development of hemodialysis membrane with chitosan and its derivative in the future.

2. Computational details

2.1. Computational analysis of density functional theory (DFT)

The theory for calculation in this study was density functional theory (DFT). Firstly, the minimum energy of chitosan, urea, and creatinine was obtained by optimization, individually. The most stable molecule of chitosan interacted with the most stable molecule of creatinine and urea to get the minimum energy of chitosan-creatinine and chitosan-urea complexes. After the optimization, the molecules and complexes have to be calculated their frequencies to clarify the molecule stability. If all frequency is positive, this molecule is stable [7,12–14,19]. Furthermore, after the complexes were optimized, the calculation of Basis Set Superposition Error (BSSE) was employed to determine the interaction energy. The following equation calculation for the interaction of energy:

$$E_{\text{int}} = E_{\text{cs/urea}} - (E_{\text{cs}} + E_{\text{urea}}) + E_{\text{BSSE cs/urea}} \quad (1)$$

$$E_{\text{int}} = E_{\text{cs/creatinine}} - (E_{\text{cs}} + E_{\text{creatinine}}) + E_{\text{BSSE cs/creatinine}} \quad (2)$$

where $E_{\text{cs/urea}}$ and $E_{\text{cs/creatinine}}$ are the minimum energies of chitosan-urea and chitosan-creatinine complexes. The interaction of both chitosan-creatinine or chitosan-urea is non-covalent. One of the non-covalent interaction is hydrogen bond interaction [28]. The determination of the interaction energy aims to determine the type of interaction of hydrogen bonds, whether weak, medium, or strong.

2.2. HOMO – LUMO energy analysis

The reactivity to transfer electron is determined by the calculation of HOMO – LUMO energy [8,10,15,16,48,60]. According to the Koopmann theorem, HOMO energy related to ionization energy (I) and LUMO energy [42] been used to estimate the electron affinity [15,48,49]. The other chemical descriptors such as chemical hardness (η),

electronegativity (χ), softness (S), global electrophilicity index, and electrophilicity index (ω), a chemical potential (μ) can be obtained from HOMO and LUMO energy by following equations:

$$I = -\text{HOMO} \quad (3)$$

$$A = -\text{LUMO} \quad (4)$$

$$\eta = \frac{1}{2}(E_{\text{LUMO}} - E_{\text{HOMO}}) \quad (5)$$

$$\chi = -\mu \approx \frac{1}{2}(I + A) \approx -\frac{1}{2}(E_{\text{HOMO}} + E_{\text{LUMO}}) \quad (6)$$

$$S = \frac{1}{\eta} \quad (7)$$

$$\omega = \frac{\mu^2}{2\eta} \quad (8)$$

HOMO energy value shows the molecular ability to donate electron in which a value higher than the E_{HOMO} value implies the increase of molecular ability to donate an electron to the acceptor. Meanwhile, E_{LUMO} shows the molecular ability to receive electron. A molecule with low E_{LUMO} can receive more electrons [40,48].

2.3. Computational analysis of Natural bond orbital (NBO) and quantum theory atom in molecule (QTAIM)

In evaluating the charge distribution, type of interactions binding energies, and reactivity to transport proton, a set of NBO calculations were employed [12,15,30,31,33–35]. Based on Second-Order Perturbation Theory, the hyper conjugative interaction energy between an occupied (i) and an unoccupied (j) NBO was calculated, as described in Eq. (9).

$$E^2 = \Delta E_{ij} = q_i \frac{F_{ij}^2}{\varepsilon_j - \varepsilon_i} \quad (9)$$

where q_i is the donor occupancy, F_{ij}^2 is the NBO Fock matrix between i and j, and $\varepsilon_j - \varepsilon_i$ is the difference between the energies of j and i NBOs [7,8,48–50,64]. The NBO method gives an accurate Lewis structure of a molecule through the highest possible percentage of an orbital electron density, becoming a useful method for analyzing intra- and intermolecular interactions [10]. Quantum Theory Atom in Molecule (QTAIM) is normally generated to support the NBO analysis [38]. QTAIM was calculated by Multiwfn software [84]. Furthermore, intrinsic strength bond strength index (IBSI) was also generated to study qualitatively the strength of hydrogen bonding. IBSI WAS a New Way for Probing Bond Strength [39]. All the calculations were performed using Gauss View graphical interface, Chemcraft [40], and NWChem [41]. The DFT method generated all calculation with the high quality of Becke three-parameter exchange; Lee et al. of correlation functional (B3LYP) method; and 6-31++g** basis set. This study also compares the gas phase, water solvent (SMD Solvation Model), and water solvent with Grimme's D3 dispersion correction. The dispersion correction in the solvent effect is generated because this is vital for the valid analysis of transport studies over the membrane and essential for agreement with experimental values [42].

3. Results and discussion

3.1. Isolated structure of chitosan dimer, urea, creatinine

The geometry monomer structure was calculated to obtain a stable molecule and minimum energy. Firstly, chitosan dimer, urea, and

creatinine structures were optimized individually using the Nwchem program. The result of the optimization geometry can be seen in Fig. 1.

Chitosan dimers were chosen to represent the chitosan polymer due to the interaction energy and enthalpies between a dimer, trimer, and oligomer with water similar [20]. Since chitosan dimer can be represented as researchers use chitosan dimer for their research [11–14,20–25]. The optimum geometry of chitosan dimer (Fig. 1) presents seven H-bonds ($a = 2.40717 \text{ \AA}$, $b = 2.65884 \text{ \AA}$, $c = 1.94862 \text{ \AA}$, $d = 2.47443 \text{ \AA}$, $e = 2.36173 \text{ \AA}$, $f = 2.62226 \text{ \AA}$, $g = 2.65661 \text{ \AA}$). The bond rotation between the pyranose rings can be evaluated by the χ dihedral angle [12]. The f and c bonds help to keep both pyranose rings in the same average plane, as can be verified by the small magnitude of the calculated χ dihedral angle. The considered chitosan conformation presents $\chi = -36.999$. The planarity of disaccharides, oligosaccharides, and chitosan polysaccharides can be determined by torsion angles φ and ψ . The φ and ψ were calculated between the bonds from each cycle of the disaccharide moiety to its glycosidic oxygen atom [7,26]. The φ and ψ angles in the optimized dimer of chitosan present values of $\varphi = -114.557^\circ$ and $\psi = -159.559^\circ$. Based on these values, it showed that chitosan dimer has great planarity between its saccharide units because the values of φ and ψ in the chitosan dimer are larger than linear protonated chitosan dimer (-114.557° and -159.559° against -96.7° and -153.8° respectively) that have been calculated by Costa et al., 2018 in the previous study [12].

Creatinine was chosen because creatinine is a toxic waste substance of creatinine phosphates [26] in muscle contraction. Normal levels of creatinine in humans is 0.7–1.2 mg/dL. Creatinine filtered by the kidneys is then excreted in the urine. The increasing concentration of

creatinine caused decreasing kidney activity [50]. To make a selective membrane for hemodialysis, we have to know the size of toxic substances that should be removed from the blood and the compound needed for our body. Creatinine and urea are the substances that have to be removed from the blood. The size of creatinine was calculated and depicted in Fig. 1. The result gave information that creatinine has a size of 5.61 Å. The size was obtained by calculating the longest distance of the molecule represented by H13.....O8.

The other toxic molecule that must be removed from the blood is urea. Urea is the final product organic compound of protein metabolism in the human body. Urea harms the body if it is excessive in the blood. Normal urea levels in humans within 15–40 mg/dL [51]. To reject the urea from the blood, the hemodialysis membrane also should have a pore size bigger than urea. The optimization of molecule urea gives information that urea has a size of 4.05 Å. According to Fig. 1, the size of the urea is smaller than creatinine.

According to the creatinine and urea size calculated in this study, it can be considered to make a membrane with a pore size bigger than creatinine or more than 5.358 Å. The other consideration to determine the good pore size of the membrane for hemodialysis is macromolecule size such as protein, hormone, immunoglobine or antibody that is important for our body, according to the study conducted by Reth et al. (2013). Immunoglobulin has a size of approximately 100 Å [52,53]. That is why the hemodialysis membrane typically ranges on the dialysis membrane to the nanomembrane, with a pore size of around 10–100 Å [54,55].

Furthermore, based on the comparison of creatinine and urea size, it can be inferred that urea easier to transport in the chitosan membrane than creatinine. This result was consistent with Lusiana, Siswanta, and

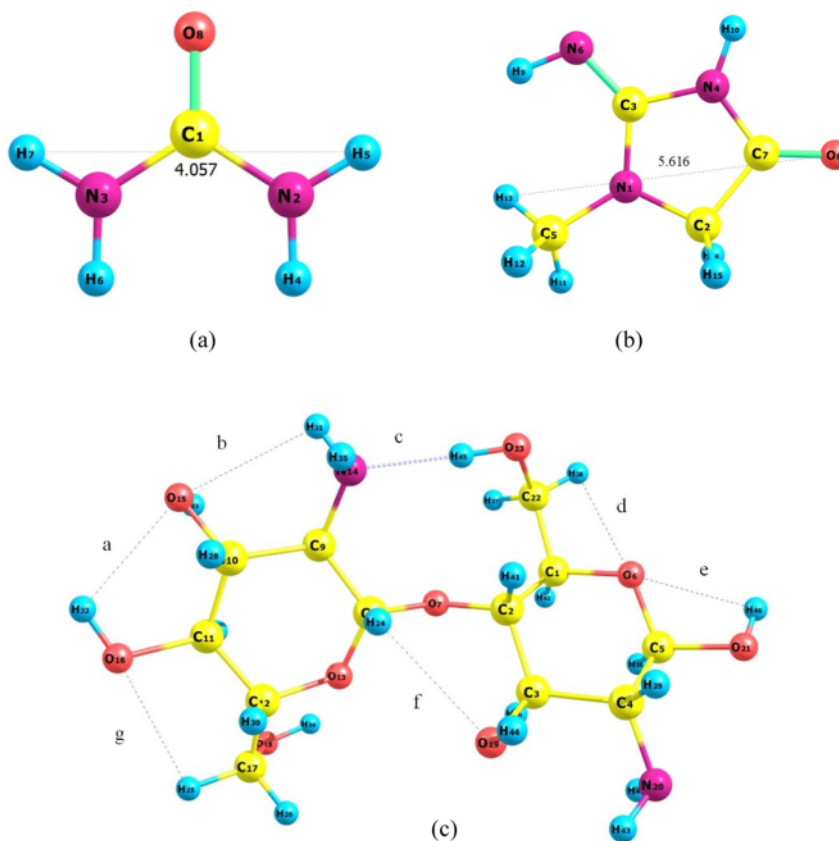


Fig. 1. Optimize geometry of molecule; (a) Urea (b) Creatinine (c) Chitosan dimer.

Table 1

The interaction energy of chitosan-creatinine and chitosan-urea.

Complexes	Solvent	Theory level	Interaction energy (kcal/mol)	Hydrogen bond
Chitosan-creatinine	Gas	B3LYP DFT/6-31 g**	−19.04	R(H34...N56) = 1.88 Å R(O13...H54) = 1.94 Å R(H44...O48) = 1.86 Å
Chitosan-creatinine	Water	B3LYP DFT/6-31 g**	−11.2	R(H34...N56) = 1.80 Å R(O13...H54) = 2.12 Å R(H44...O48) = 1.81 Å
Chitosan-creatinine	Water	B3LYP DFT-D2/6-31 g**	−20.68	R(H34...N56) = 1.77 Å R(O13...H54) = 1.97 Å R(H44...O48) = 1.76 Å
Chitosan-creatinine	Water	B3LYP DFT-D2/6-31++g**	−14.14	R(H34...N56) = 1.83 Å R(O13...H54) = 1.94 Å R(H44...O48) = 1.78 Å
Chitosan-creatinine	Water	B3LYP DFT-D3/6-31++g**	−13.50	R(H34...N56) = 1.81 Å R(O13...H54) = 2.00 Å R(H44...O48) = 1.80 Å
Chitosan-urea	Gas	B3LYP DFT/6-31 g**	−10.62	R(H54...O13) = 2.76 Å R(H55...O19) = 1.96 Å R(O48...H47) = 2.34 Å
Chitosan-urea	Water	B3LYP DFT/6-31 g**	−3.98	R(H54...O13) = 2.78 Å R(H55...O19) = 2.04 Å R(O48...H47) = 2.36 Å
Chitosan-urea	Water	B3LYP DFT-D2/6-31 g**	−9.93	R(H54...O13) = 2.76 Å R(H55...O19) = 1.96 Å R(O48...H47) = 2.34 Å
Chitosan-urea	Water	B3LYP DFT-D2/6-31++g**	−8.40	R(H54...O13) = 2.81 Å R(H55...O19) = 1.98 Å R(O48...H47) = 2.53 Å
Chitosan-urea	Water	B3LYP DFT-D3/6-31++g**	−4.76	R(H54...O13) = 3.02 Å R(H55...O19) = 2.10 Å R(O48...H47) = 2.76 Å

Hayashita's studies (2013) that urea has higher % transport in the chitosan derivative membrane than creatinine [4]. The pore size and permeation size are not only the factor of the membrane ability to transport creatinine or urea. The other factor is hydrogen bonding [6]. Therefore more detail about hydrogen bonding between chitosan and creatinine or urea will be further discussed.

3.2. Interaction energy

Intermolecular interaction is a study to understand how atoms and molecules are organized within a system of chemistry [32–37]. Several publications have demonstrated that chitosan and its derivatives form stable complexes with proteins and peptides to find an effective drug delivery method [8,38,39]. A high value of interaction energy (E_{int}) describes a strong binding between the two molecules, while a decrease in E_{int} facilitates dissociation of a molecule. The interaction study can also explain the interactions in the membrane transport phenomena with a molecule in the solutions. One example in several publications was evaluated proton and electron transfer on the Proton Exchange Membrane Fuels Cells, which described cellulose interaction with water molecules [32]. The binding affinity of hydrogen bond was evaluated at the B3LYP-D3/6-31++G** level and corrected by zero-point energy (ZPE) and basis set superposition error (BSSE). Furthermore, these calculations were also simulated in the gas phase, intrinsic solvent effect with SMD solvation model, and dispersion effect in the water solvent (Table 1).

The interaction energy of chitosan-creatinine simulated in the gas phase is about −19.04 kcal/mol. This energy is higher than in the water solvation model by approximately −11.20 kcal/mol due to the creatinine is highly solvated in the water and made the hydrogen bond interacts with water. This data are also similar to several publications in which, in their study, the interaction in the water solvent is weaker than in the gas phase [23,25,42]. In contrast, the water solvent

simulation corrected with dispersion (D2) effect presents the highest interaction energy around −20.68 kcal/mol. Hence, This study emphasizes the contribution of Vanderwaal's interactions in the transport process, where dispersion interaction is one of Vanderwaal's interactions component. Singla et al. (2016) reinforced that the interaction energy calculated by including dispersion correction deemed the process to be exergonic, which implied that the interaction is loveable electronically. Furthermore, B3LYP/DFT-D3 and diffuse basis set 6-31++g** were also employed to get more accurate calculations close to the real experiment. The result shows that the interaction energy between chitosan and creatinine is about 13.50 kcal/mol. Then, Fig. 2 also shows that the hydrogen bonds on the chitosan-creatinine interaction occur in R (H34...N56) = 1.81 Å R(O13...H54) = 2.00 Å R(H44...O48) = 1.80 Å. Furthermore, the data shows that the average lengths were under 2.0 Å and more than 1.8 Å. These data were classified as medium hydrogen bonds [32].

The calculation of interaction energy value of chitosan-urea complexes was −10.61 kcal/mol in the gas phase, −3.90 kcal/mol in water solvent −9.93 kcal/mol in water solvent corrected dispersion (D2) effect. This data depicts that the interaction in solvent water without dispersion correction has the energy more positive than the solvent model corrected with dispersion effect because the interaction energy generated without dispersion effect is more endergonic [42,64]. Moreover, The interaction energy between chitosan and urea simulated on B3LYP/DFT-D using a diffuse basis set 6-31++g** is about −4.76 kcal/mol. Then, Fig. 2b illustrated that There are three hydrogen bond interactions among chitosan and urea that consist of: R(H54...O13) = 3.02 Å R(H55...O19) = 2.10 Å R(O48...H47) = 2.76 Å. According to the data of interaction energy and distance in the hydrogen bond shown in Table 1, this interaction was the medium hydrogen bond type.

Identifying hydrogen bond strength between the target molecule and the functional group on the membrane is important because it

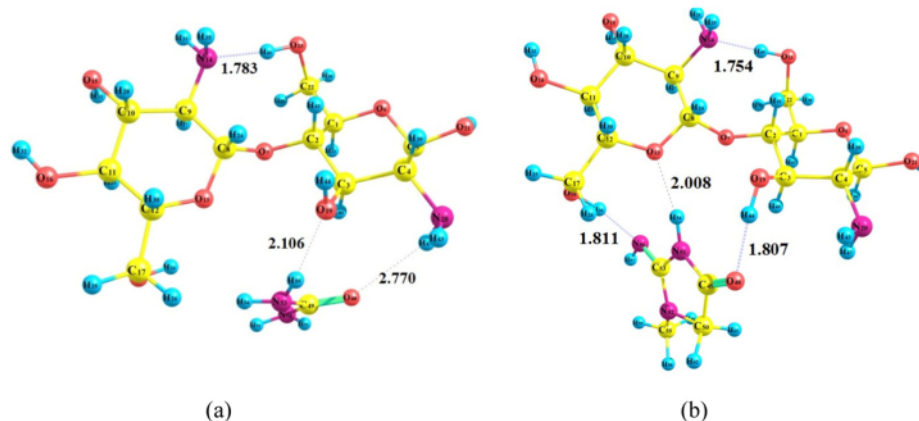


Fig. 2. Simulation in DFT-D3 B3LYP 6-31++g** (a) Chitosan dimer-urea interaction (b) Chitosan dimer-creatinine interaction.

Table 2

The chemical descriptor of the system.

System	E HOMO	E LUMO	I	A	η	S	μ	χ	ω
Chitosan	−6.2124	1.0803	6.21241	−1.0803	7.29271	0.13712	−2.5661	2.56605	0.45145
Urea	−6.6315	1.64358	6.63147	−1.6436	8.27505	0.12085	−2.4939	2.49394	0.37581
Creatinine	−6.3104	0.07347	6.31037	−0.0735	6.38384	0.15665	−3.1184	3.11845	0.76167
Chitosan-urea	−5.7553	0.94968	5.75525	−0.9497	6.70494	0.14914	−2.4028	2.40278	0.43053
Chitosan - creatinine	−5.8042	−0.6885	5.80423	0.68845	5.11578	0.19547	−3.2463	3.24634	1.03002

can affect the molecular target permeability to the membrane [3,7,65]. The strong hydrogen bond interaction energy usually is more than 20 kcal/mol, where the strong hydrogen bond can accelerate transport in the membrane [7]. However, the strong hydrogen bond can also make fouling in the membrane. On the other hand, the membrane with a weak hydrogen bond interaction (under 4 kcal/mol) with urea and creatinine will have slower action to transport these molecules than medium or strong hydrogen bonds [41–46]. Thus, the medium hydrogen bond is the best interaction for the membrane to increase transport creatinine and urea. The range of interaction energy for the medium hydrogen bond interaction is between 4 kcal/mol and 20 kcal/mol [32]. Based on this finding implied that chitosan is a critical and potential material for transport urea and creatinine.

Taking into consideration, These results reinforced the creatinine molecule interacted with the chitosan dimer stronger than urea. These data can be concluded that creatinine is easier to be transported than urea in the chitosan membrane. Although the creatinine interacts stronger in chitosan than urea, the value of interaction energy almost similar. It means that both chitosan and creatinine have the same probabilities of transporting in the chitosan membrane. The interaction energy and the particle size are not always the parameter in the transport phenomenon [48,49]. The other parameter is proton transfer; electron transfer; energy stabilization; reactivity of chitosan, urea, and creatinine.

3.3. Reactivity of model system

Molecular orbitals' theoretical approaches are useful in predicting the reactivity of molecules [29]. The quantum chemical parameters to explain the activity of molecule are ionization energy (I), electron affinity (A), chemical hardness (η), electronegativity (χ), softness (S), global electrophilic index (ω), and chemical potential (μ). They used the quantum chemical parameters to determine the HOMO and LUMO energy [8,10,25,49–54]. Molecular orbital (HOMO) is related to the ability to donate electron capacity of molecules, whereas molecular orbital (LUMO) indicates the electron-accepting ability [31]. All the data of chemical descriptors on the system is presented in Table 2.

Chemical hardness (η) is defined as the molecular resistance needed to deform the number of electrons correlated with the stability and reactivity of a chemical system [74]. A rigid molecule has a high HOMO-LUMO gap. The more massive gap means that a molecule is more stable. Table 2 shows that creatinine has a lower chemical hardness than urea, which implies that creatinine is more reactive than urea.

The electronegativity data gave information that creatinine has a higher electronegativity than urea, which implies that creatinine was more electrophilic than urea. According to this data, it can be determined that creatinine was more electrophilic, while chitosan and urea are more nucleophilic. Creatinine is more electrophilic than urea because there is a steric effect in the cyclic of creatinine that inhibit the nucleophile functional group in the creatinine molecule, while urea has no steric effect. The steric effect can be seen in Fig. 6. The best membrane is the membrane that has a difference in electrophilicity. Hence the membrane can attract the molecular target. According to this data, the creatinine can make a stronger bonding with chitosan than urea because urea has almost similar electrophilicity with chitosan. This data is similar to the interaction energy where chitosan-creatinine has higher interaction energy than chitosan-urea.

In the other data, HOMO-LUMO gap in this study aimed to understand the ability of chitosan-creatinine and chitosan-urea to transfer electrons. The molecule or complex with a small HOMO-LUMO gap interpreted that this molecule was easier to transfer electron and more reactive [75–79]. The HOMO-LUMO gaps were presented in Fig. 3.

Fig. 3 shows that both creatinine and urea caused decreasing the HOMO-LUMO energy gap on chitosan. Fig. 3 informs that the bandgap of chitosan-creatinine and chitosan-urea are 5.11 eV and 6.70 eV, respectively. The interaction of chitosan-creatinine showed a decrease in the energy gap was significant compared to the bandgap of the chitosan dimer. Whereas, in the interaction of chitosan-urea, only small decreases. Based on previous research, the smaller gap energy HOMO-LUMO means the unstable molecules [55–59]. The compound instability only takes a small amount of energy to the electron can be excited from the HOMO to LUMO. chitosan-creatinine and chitosan-urea complexes have a similar HOMO energy, but the LUMO energy of chitosan-creatinine complex was lower than chitosan-urea complex. "This data

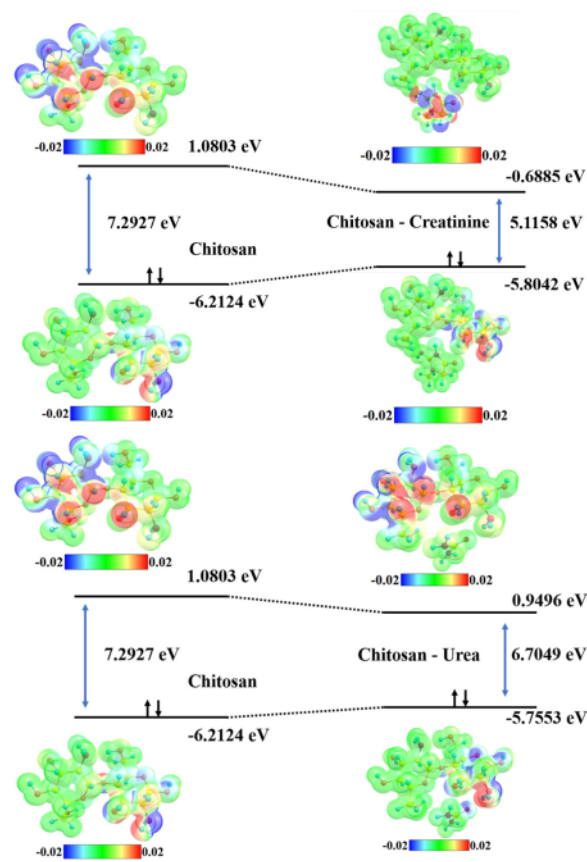


Fig. 3. HOMO-LUMO gap energy of a. Chitosan dimer-creatinine b. Chitosan dimer-urea.

Table 3
NBO analysis of chitosan dimer-creatinine.

No	Donor (L) NBO	Acceptor (NL) NBO	E(2) (kcal/mol)	E(NL)-E(L) (a.u.)	F(L,NL) (a.u.)
Chitosan to creatinine					
1	LP (1) O 13	178. BD*(1) N 51- H 54	3.59	0.91	0.051
2	LP (2) O 13	178. BD*(1) N 51- H 54	9.32	0.82	0.078
Creatinine to chitosan					
3	LP (1) O 48	162. BD*(1) O 19- H 44	5.87	1.06	0.07
4	LP (2) O 48	162. BD*(1) O 19- H 44	10.71	0.78	0.082
5	LP*(1) N 56	161. BD*(1) O 18- H 34	18.02	0.83	0.109
6	BD (2) C 53- N 56	161. BD*(1) O 18- H 34	1.83	0.84	0.035

demonstrated that both chitosan-creatinine and chitosan-urea complexes have the same ability to donor electron but difference to accept an electron". However, both creatinine and urea can decrease the individual chitosan bandgap, causing the transferred electron to be more accessible. Thus, this data suggests that chitosan can be determined as the potential candidate to be hemodialysis membrane.

3.4. NBO analysis

The determination of hydrogen bond interaction is crucial for study interaction, especially for transport phenomena. Energy interaction is not enough to judge the strength of hydrogen bonding interaction. The other theoretical approach is by NBO analysis. NBO analysis normally used to study deeply about the natural orbital that primarily involve in the Hydrogen bonding interaction [80]. The NBO analyses point to the formation of H-bonds within the chitosan dimer and urea or creatinine.

Table 3. shows the presence of hydrogen bond between chitosan-creatinine at atom O18-H34...N56 with the stabilization energy of 18.02 kcal/mol, which is classified as the medium hydrogen bond interaction. Kwan (2009) supported this finding that medium hydrogen bonds have stabilization energy more than 4 kcal/mol and less than 20 kcal/mol [81]. The stronger hydrogen bonds will be easier to transfer protons. Thus, it can be concluded that it would be accessible to creatinine in the transport mechanism. The complex of chitosan-urea containing hydrogen bonds with stabilization energy only revolves around 3.07 kcal/mol - 4.34 kcal/mol. Hydrogen bonds occur in O18...H54-N53, O19...H55-N53, O48...H47-N20 (see in Table 4 and Fig. 2). Although hydrogen bonds occur at the atom with high electronegativity, the stabilization energy was less than 11.24 kcal/mol. It indicated that hydrogen bond interaction that occurs in the complex of chitosan-urea was not strong enough. The lower stabilization energy means that more weak hydrogen bond interaction causes difficulty transferring protons [47,49]. Therefore, it can be presumed that the interaction of hydrogen bonds of chitosan-urea is weaker than chitosan-creatinine.

Table 4
NBO analysis of chitosan dimer-urea.

No	Donor (L) NBO	Acceptor (NL) NBO	E(2) (kcal/mol)	E(NL)-E(L) (a.u.)	F(L,NL) (a.u.)
Chitosan urea					
1	LP (2) O 13	BD*(1) N 53- H 54	4.34	0.79	0.052
2	LP (1) O 19	BD*(1) N 53- H 55	4.07	1.01	0.057
3	LP (2) O 19	BD*(1) N 53- H 55	4.32	0.84	0.054
Urea chitosan					
4	LP (1) O 48	BD*(1) N 20- H 47	3.32	1.05	0.053
5	LP (2) O 48	BD*(1) N 20- H 47	3.07	0.76	0.043

3.5. Quantum theory atom in molecule QTAIM

Bader (1990) has introduced the theory of QTAIM in a molecule for the first time. This theory uses the distribution of electron density between two atoms to explain a system of chemical structure. Bader described bond critical point (BCP) as a saddle point of electron density between two atoms that form a chemical bond [82]. QTAIM analysis can give useful parameters such as Laplacian (representing the local charge concentration or depletion) and ellipticity (the measure of "double bond" or π character). The equation of Laplacian parameters at the BCP is given by

$$\nabla^2\rho = \lambda_1 + \lambda_2 + \lambda_3,$$

where λ_1, λ_2 , and λ_3 are three parameters of the density at the critical point. To help more accurate data, Electronic energy density (H) can be determined by the following equation

$$H_{(BCP)} = G_{(BCP)} + V_{(BCP)}$$

$G_{(BCP)}$ is kinetic energy density, and $V_{(BCP)}$ is potential energy density. Now, The type of interaction can be identified with $\nabla^2\rho$, and $H_{(BCP)}$.

$\nabla^2\rho$ (+) and $H_{(BCP)}$ (+) The weak covalent interactions (strong electrostatic bond).

$\nabla^2\rho$ (-) and $H_{(BCP)}$ (-) Strong interaction (strong covalent bond), $\nabla^2\rho$ (+) and $H_{(BCP)}$ (-) medium strength (partially covalent bond).

On the other hand, the ratio of $|V/G|$ is a reliable parameter to classify the different interactions. According to this parameter, weak interactions are described with $|V/G| < 1$, medium interactions $1 < |V/G| < 2$, and strong interactions $|V/G| > 2$.

In this research, multiwfn software was applied to calculate The values of kinetic energy density (G), potential energy density (V), Laplacian ($\nabla^2\rho$), total energy density (H), and the ratio of $|V/G|$. These parameters were listed in Table 4. The BCP plots for the interaction of chitosan-creatinine and chitosan urea-are shown in Fig. 43

The BCP for the interaction of chitosan-creatinine can be seen in Fig. 4. According to Fig. 4, it showed that there is four necessary BCP in the creatinine or urea. The analytical data for the BCP is presented in Table 5.

On the complex chitosan-creatinine, there is three BCP (16, 19, 27, 51), which have a negative value for $H_{(BCP)}$ and positive value for $\nabla^2\rho$. Base on that, data informs which the BCP includes in the medium interaction or partial interaction. The ratio of $|V/G|$ in that BCP is $1 < |V/G| < 2$, which meant that the interaction between chitosan and creatinine is medium interaction (medium hydrogen bond). Positive $\nabla^2\rho$ and $H_{(BCP)}$ values and $|V/G| < 1$ in the BCP (80) denote the weak covalent interactions (strong electrostatic bond). The QTAIM analysis in the complex chitosan-creatinine can be concluded to have three hydrogen bonds.

Analysis QTAIM in the chitosan-urea also has already operated with multiwfn software. The hydrogen bond occurs in the BCP with index 86, 91, 110, and 119. The BCP (86,91, 110, and 119) have negative $H_{(BCP)}$ and positive $\nabla^2\rho$ value which refer to medium interaction (medium

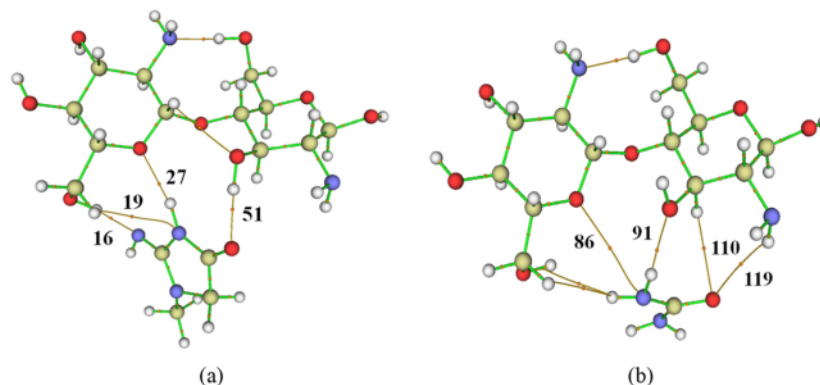


Fig. 4. Bond critical point index for (a) Chitosan-creatinine, (b) Chitosan-urea.

Table 5
The QTAIM parameters.

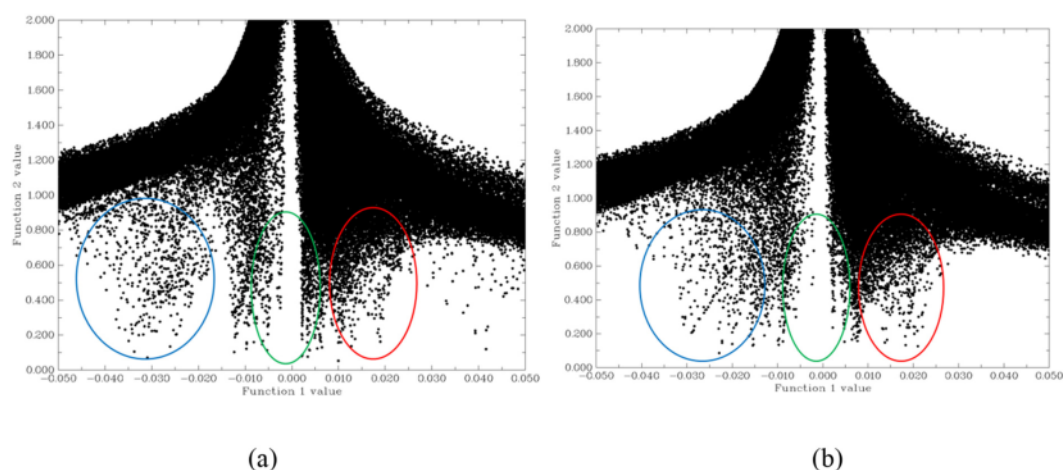
BCP	$\rho(\text{BCP})$	$\nabla^2\rho$	$G(\text{BCP})$	$H(\text{BCP})$	$-V(\text{BCP})$	$ V/G $	λ_1	λ_2	λ_3	$E(\text{BCP})$	EHB (kcal/mol)
Chitosan-creatinine											
16	0.0398	0.0924	0.0249	−0.0018	0.0266	1.0712	0.0443	0.0491	−0.0010	0.0689	−8.3565
19	0.0051	0.0191	0.0037	0.0011	0.0026	0.7102	0.0017	0.0168	0.0005	1.2170	−0.8238
27	0.0223	0.0610	0.0160	−0.0007	0.0167	1.0449	0.1041	−0.0155	−0.0275	0.0616	−5.2382
51	0.0346	0.1017	0.0256	−0.0002	0.0257	1.0064	0.1830	−0.0373	−0.0440	0.0238	−8.0788
Chitosan-urea											
86	0.0041	0.0146	0.0031	0.0006	0.0025	0.8099	0.0119	0.0052	−0.0024	0.6028	−0.7816
91	0.0172	0.0529	0.0134	−0.0001	0.0135	1.0075	0.0618	−0.0149	0.0060	0.1012	−4.2357
110	0.0077	0.0253	0.0056	0.0007	0.0049	0.8685	0.0349	−0.0046	−0.0050	0.0588	−1.5222
119	0.0050	0.0187	0.0038	0.0009	0.0028	0.7561	0.0082	0.0051	0.0055	0.1241	−0.8928

hydrogen bond). This data also supported with $|V/G|$ ratio, which has value $1 < |V/G| < 2$. The BCP with index 111 has a positive $H(\text{BCP})$ and $\nabla^2\rho$ value which meant the weak covalent interactions (strong electrostatic bond). Despite a weak covalent interaction, the average interaction between chitosan and urea is medium interaction (medium hydrogen bond).

The Hydrogen bond energy (E_{HB}) also determine in this analysis. The average value of hydrogen bond energy in all complexes is 4–10 kcal/mol, which is included in the medium hydrogen bond. The hydrogen bond energy in the complex chitosan-creatinine bigger than chitosan-urea. According to this data strongly conclude that creatinine has a

stronger attraction with chitosan than urea. This data is also supported by all of the data in this research.

On the other hand, This data also demonstrated that chitosan is a potential candidate as a hemodialysis membrane because it can make a medium hydrogen bond with urea and creatinine. Compared to Polysulfone, Chitosan has a stronger interaction with urea and creatinine. The interaction of polysulfone with urea and creatinine had been calculated by Sasongko et al. (2020). That study showed that Polysulfone has E_{HB} by about 0.02–2.98 kcal/mol [7]. It implies that chitosan has a better interaction with urea and creatinine than a clinical membrane-based polysulfone.

Fig. 5. The RDG/ $\text{sign}(\lambda_2)\rho$ for (a) chitosan-creatinine (b) chitosan-urea.

3.6. Reduced density gradient (RDG) and NCI index

The intramolecular interactions and the nature of the weak interactions on chitosan-creatinine and chitosan-urea have been evaluated by plotting the non-covalent interaction (NCI) index and the reduced density gradient (RDG). The NCI index gives more information related to the non-covalent interaction, such as hydrogen bond. The reduced density gradient (RDG) is defined as (Johnson et al. 2010):

$$RDG(r) = \frac{1}{2(3\pi^2)^{1/3}} \frac{|\nabla\rho(r)|}{\rho(r)^{4/3}}$$

The value of RDG characterizes the non-covalent interaction of complexes. Fig. 5. showed the scatter graphs of RDG versus $\text{sign}(\lambda_2)\rho(r)$ for all complexes. Multiwfn program was used to obtained The sign $(\lambda_2)\rho(r)$ and NCI–RDG plots [83]. The value of λ_2 and ρ can utilize to analyze the interaction type.

$\lambda_2\rho < 0$ and $\rho > 0$ means that strong attraction (hydrogen bond, halogen bond).

$\lambda_2\rho \approx 0$ and $\rho \approx 0$ Van der Waals interaction.

$\lambda_2\rho > 0$ and $\rho > 0$ Strong repulsion (steric effect in-ring and cage).

The RDG scatter graph blue color circle shows the Hydrogen bond, the red color circle denotes the steric effect, and the green circle corresponding to Van der Waals interactions. Fig. 5 showed that all of the complexes have medium hydrogen bonds shown in the blue color circle. Furthermore, the diagram density of chitosan-creatinine complex in the blue area is denser and more negative than chitosan-urea complexes. Thus, this data illustrated that the formation of hydrogen on chitosan-creatinine is stronger than creatinine-urea. Fig. 6 performed the more real imagination to explain the scatter graphs of RDG versus $\text{sign}(\lambda_2)\rho(r)$, where Fig. 6 illustrates the location of hydrogen bonds, van der Waals, and steric effect. Fig. 6. display the isosurface of complex Chitosan-urea and Chitosan-creatinine. It can be shown that chitosan formed a hydrogen bond both with urea and creatinine. A previous study conducted by Sasongko, 2020 found that PSf as an approved hemodialysis membrane did not make a hydrogen bond with urea and creatinine or only Van der Waals forces [7]. Hence, this indicates that chitosan

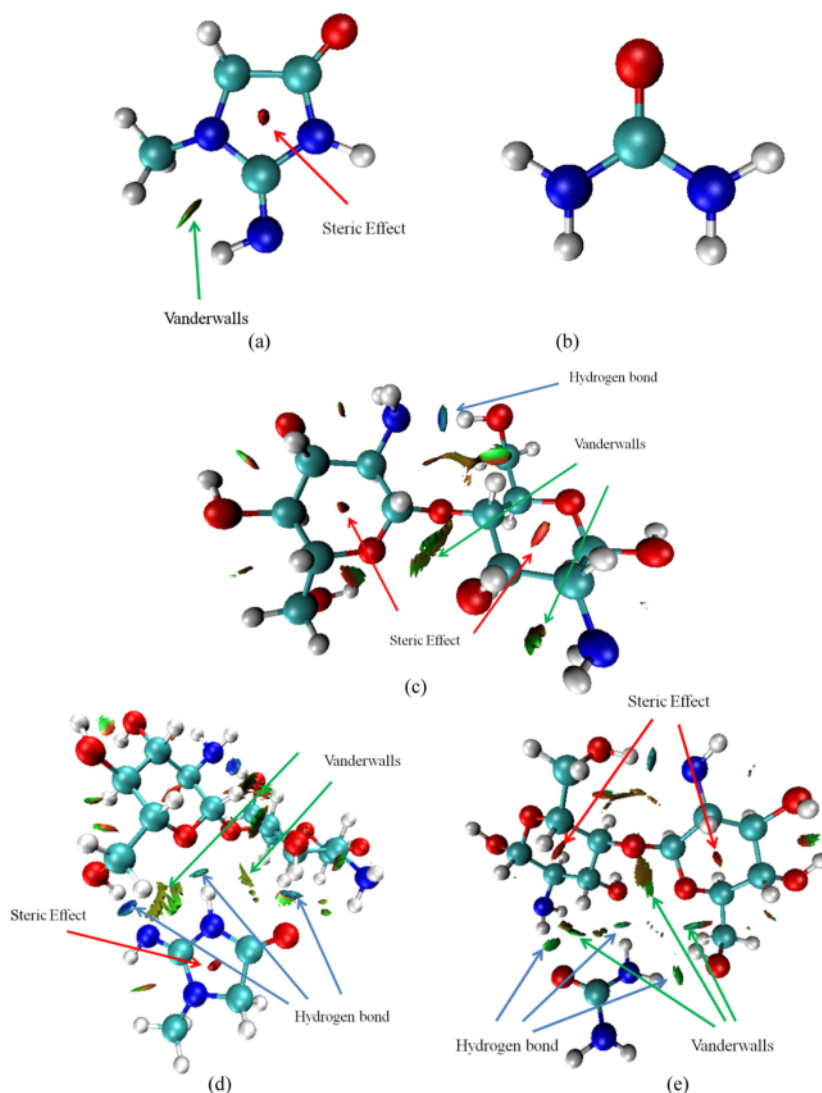


Fig. 6. RDG isosurface for (a) creatinine (b) urea (c) chitosan (d) chitosan-creatinine (e) chitosan-urea.

is a potential molecule for the hemodialysis membrane compared to PSF. Furthermore, Fig. 6. Also, support the chemical parameters data where urea has no steric effect while chitosan and creatinine have a steric effect.

3.7. Intrinsic bond strength index (IBSI)

In 2020, a new approach was enlarged able to assess the most relevant atomic contributions to the non-covalent interactions occurring between two fragments. This development proves to be an appealing tool to shed light on the guest accommodation on a per-atom basis. Also, in 2020 the new Intrinsic Bond Strength Index IBSI was initiated. IBSI score give very efficient data to internally probe the strength given by atom pair, over a wide range (non-covalent to covalent). An IBSI scale has been developed to range two-centre chemical bonds by their intrinsic strength. In 2020 was, Klein et al proposed a new release allowing for detecting the interaction between two given sub-fragments of a single molecule, using QM electron density [39]. This probability is particularly engaging to evaluate the role of non-covalent intramolecular interactions such as intramolecular π - π stacking and hydrogen-bonding [39]. In this study, IBSI was calculated to evaluate quantitatively the strength of intermolecular hydrogen bond on chitosan-creatinine, and chitosan-urea complexes. The IBSI data was presented in Table 6.

Table 6. shows that the chitosan-creatinine complex has an IBSI by about 0.117 on average, while chitosan-urea complex only has an IBSI under 0.1. Moreover, Klein et al (2020) classified that hydrogen bond is generally ≤ 0.15 on the IBSI scale and larger than 0.053 [39]. According to that range and Table 6., it can be implied that Creatinine forms 3 hydrogen bond with chitosan while only 1 hydrogen bond that is created from the interaction between chitosan and urea. Furthermore, The location of intermolecular hydrogen bond interaction was depicted on the (Supplementary file, Figs. 2 and 3). Furthermore, IBSI analysis also separated the contribution of inter and intramolecular hydrogen bond interaction that is not shown in the RDG and NCI analysis. Overall, The IBSI data shows that chitosan.

4. Conclusion

In this work, the formation of chitosan-creatinine and chitosan-urea complexes was evaluated by structure optimizations. Intramolecular H-bonds kept the optimized structures of the isolated chitosan dimer. The size of creatinine and urea were 5.358 Å and 4.057 Å, respectively. The interaction between urea or creatinine and chitosan dimer existed as medium hydrogen bond interactions. The interaction energy structures of chitosan-creatinine are higher than chitosan-urea complexes. The chemical reactivity parameter proved that creatinine is more electrophilic than urea, making it easier to interact with chitosan less electrophilic. Both creatinine and urea can decrease the gap energies of chitosan dimer. The energy gap of HOMO-LUMO of complex chitosan-creatinine was lower than complex chitosan-urea. It can be concluded that chitosan-creatinine was more reactive than chitosan-urea. The energy gap complexes can give the future pathway to develop the hemodialysis membrane, which involved photo-electric to accelerate the

small molecular transports. The result of NBO analysis showed a high contribution of a hydrogen bond between chitosan-creatinine and chitosan-urea. The chitosan-creatinine has a stronger hydrogen bond than chitosan-urea through the interaction O18-H34...N56 with stabilizing energy = -13 kcal/mol. AIM analysis data also support the NBO data. Thus, chitosan functional groups can help transport urea and creatinine by hydrogen bond interactions through -NH₂ and -OH groups. All data also showed that chitosan more favorable interacted with creatinine than urea.

CRedit authorship contribution statement

Parsaoran Siahaan: Conceptualization, Formal analysis, Funding acquisition, Investigation, Methodology, Software, Project administration, sources, Supervision, Validation **Nurwarrohan Andre Sasongko:** Conceptualization, Data curation, Formal analysis, Investigation, Methodology, Resources, Validation, Visualization, Roles/Writing – original draft, Writing – review & editing, Software. **Retno Ariadi Lusiana:** Conceptualization, Validation. **Vivitri Dewi Prasasty:** Validation, Visualization, Writing – review & editing. **Muhamad Abdulkadir Martoprawiro:** Validation, Writing – review & editing.

Declaration of competing interest

The authors declare no conflict of interest.

Acknowledgement

Gratefully acknowledge to Faculty Sains and Mathematics Diponegoro University which has funded this research and technology through the non-APBN research funding scheme 2019 (No.4842/UN7.5.8/PP/2019) and 2020 (No.2005/UN7.5.8/PP/2020).

Appendix A. Supplementary data

Supplementary data to this article can be found online at <https://doi.org/10.1016/j.ijbiomac.2020.12.052>.

References

- [1] V.A. Luyckx, M. Tonelli, J.W. Stanifer, The global burden of kidney disease and the sustainable development goals, *Bull. World Health Organ.* 96 (2018) 414–422C, <https://doi.org/10.2471/BLT.17.206441>.
- [2] S.S. Hayek, S. Sever, Y.A. Ko, H. Trachtman, M. Awad, S. Wadhvani, M.M. Altintas, C. Wei, A.L. Hottot, A.L. French, L.S. Sperling, S. Lerakis, A.A. Quyyumi, J. Reiser, Soluble urokinase receptor and chronic kidney disease, *N. Engl. J. Med.* 373 (2015) 1916–1925, <https://doi.org/10.1056/NEJMoA1506362>.
- [3] R.A. Lusiana, V.D.A. Sangkota, N.A. Sasongko, G. Gunawan, A.R. Wijaya, S.J. Santosa, D. Siswanta, M. Mudasir, M.N.Z. Abidin, S. Mansur, M.H.D. Othman, Permeability improvement of polyethersulfone-polyethylene glycol (PEG-PES) flat sheet type membranes by tripolyphosphate-crosslinked chitosan (TPP-CS) coating, *Int. J. Biol. Macromol.* 152 (2020) 633–644, <https://doi.org/10.1016/j.ijbiomac.2020.02.290>.
- [4] R.A. Lusiana, D. Siswanta, Mudasir, T. Hayashita, The influence of PVA/citric acid/chitosan membrane hydrophilicity on the transport of creatinine and urea, *Indones. J. Chem.* 13 (2013) 262–270.
- [5] R.A. Lusiana, V.D.A. Sangkota, N. Andre Sasongko, S.J. Santosa, M.H.D. Othman, Chitosan based modified polymers designed to enhance membrane permeation capability, *IOP Conf. Ser. Mater. Sci. Eng.* 509 (2019), doi:<https://doi.org/10.1088/1757-899X/509/1/012122>.
- [6] R.A. Lusiana, D. Siswanta, Mudasir, Preparation of citric acid crosslinked chitosan/poly (Vinyl alcohol) blend membranes for creatinine transport, *Indones. J. Chem.* (2016) 144–150, doi:[10.14499/ijc-v16i2p144-150](https://doi.org/10.14499/ijc-v16i2p144-150).
- [7] N.A. Sasongko, P. Siahaan, R.A. Lusiana, V. Prasasty, Understanding the interaction of polysulfone with urea and creatinine at the molecular level and its application for hemodialysis membrane, *J. Phys. Conf. Ser.* 1524 (2020) 12084, <https://doi.org/10.1088/1742-6596/1524/1/012084>.
- [8] R.A. Lusiana, V.D.A. Sangkota, S.J. Santosa, Chitosan succinate/PVA-PEG Membrane: Preparation, Characterization and Permeation Ability Test on Creatinine, *J. Kim. Sains Dan Apl.* 21 (2018) 80, doi:[10.14710/jksa.21.2.80-84](https://doi.org/10.14710/jksa.21.2.80-84).
- [9] D. Dehnad, H. Mirzaei, Z. Emam-Djomeh, S.M. Jafari, S. Dadashi, Thermal and antimicrobial properties of chitosan-nanocellulose films for extending shelf life of ground meat, *Carbohydr. Polym.* 109 (2014) 148–154, <https://doi.org/10.1016/j.carbpol.2014.03.063>.

Table 6

Intrinsic bond strength index of chitosan - creatinine and chitosan - urea.

Fragment 1	Fragment 2	Distance	$f\sigma_{\text{g}}^{\text{pair}}$	IBSI ^{GHM}	IBSI ^{GM}
Chitosan-creatinine					
34(H)	56(N)	1.8106	0.20992	0.04851	0.15606
13(O)	54(H)	2.0081	0.05281	0.02615	0.11523
44(O)	48(O)	1.8072	0.06997	0.04278	0.18836
Chitosan-urea					
13(O)	54(H)	3.0206	0.01198	0.00262	0.01088
19(O)	55(H)	2.1058	0.04094	0.01843	0.08302
47(H)	48(O)	2.7697	0.01777	0.00463	0.01593

- [10] L. Li, C. Wu, Z. Wang, L. Zhao, Z. Li, C. Sun, T. Sun, Density functional theory (DFT) and natural bond orbital (NBO) study of vibrational spectra and intramolecular hydrogen bond interaction of L-ornithine-L-aspartate, *Spectrochim. Acta A Mol. Biomol. Spectrosc.* 136 (2015) 338–346, <https://doi.org/10.1016/j.saa.2014.08.153>.
- [11] S. Islam, M.A.R. Bhuiyan, M.N. Islam, Chitin and chitosan: structure, properties and applications in biomedical engineering, *J. Polym. Environ.* 25 (2017) 854–866, <https://doi.org/10.1007/s10924-016-0865-5>.
- [12] M.P.M. Costa, L.M. Prates, L. Baptista, M.T.M. Cruz, I.L.M. Ferreira, Interaction of poly-electrolyte complex between sodium alginate and chitosan dimers with a single phosphate molecule: a DFT and NBO study, *Carbohydr. Polym.* 198 (2018) 51–60, <https://doi.org/10.1016/j.carbpol.2018.06.052>.
- [13] P. Siahaan, N.E. Darmastuti, S. Aisyafalah, N.A. Sasongko, D. Hudiyantri, M. Asy'ari, V.D. Prasasty, Probing the interaction between EC1–EC2 domain of E-cadherin with conformational structure of cyclic ADTC7 (Ac-CDTPDC-NH2) peptide using molecular docking approach, *J. Phys. Conf. Ser.* 1524 (2020) 12081, doi:<https://doi.org/10.1088/1742-6596/1524/1/012081>.
- [14] J.B.L. Martins, R.P. Quintino, J.R. do S. Politi, D. Sethio, R. Gargano, E. Kraka, Computational analysis of vibrational frequencies and rovibrational spectroscopic constants of hydrogen sulfide dimer using B3LYP/2 and CCSD(T), *Spectrochim. Acta - Part A Mol. Biomol. Spectrosc.* 239 (2020) 1–9, doi:<https://doi.org/10.1016/j.saa.2020.118540>.
- [15] B.C. Deka, P.K. Bhattacharyya, DFT study on host-guest interaction in chitosan-amino acid complexes, *Comput. Theor. Chem.* 1110 (2017) 40–49, <https://doi.org/10.1016/j.comptc.2017.03.036>.
- [16] E.M. Widen, G. Strain, W.C. King, W. Yu, S. Lin, B. Goodpaster, J. Thomson, A. Courcouas, A. Pomp, D. Gallagher, Validity of bioelectrical impedance analysis for measuring changes in body water and percent fat after bariatric surgery, *Obes. Surg.* 24 (2014) 847–854, <https://doi.org/10.1007/s11695-014-1182-5>.
- [17] L.A. Juárez-Morales, Hernández-Cocolezzi*, E. H. Chigo-Anota, E. Aguila-Almanza, M.G. Tenorio-Arvide, Chitosan-Aflatoxins B1, M1 Interaction: A Computational Approach, *Curr. Org. Chem.* 21 (2017) 7.
- [18] P. Siahaan, S.N.M. Salimah, M.J. Sipangkar, D. Hudiyantri, M.C. Djunaidi, M.D. Lakstoriini, Ab Initio Computational Study of -N-C and -O-C Bonding Formation: Functional Group Modification Reaction Based Chitosan, in: *IOP Conf. Ser. Mater. Sci. Eng.* IOP, Semarang, 2018, <https://doi.org/10.1088/1757-899X/349/1/012049>.
- [19] W. Plazinski, M. Drach, Calcium- α -L-gulonate complexes: Ca²⁺ binding modes from DFT-MD simulations, *J. Phys. Chem. B* 117 (2013) 12105–12112, <https://doi.org/10.1021/jp405638k>.
- [20] I. Onoka, Geometrical Structure, Vibrational Spectra and Thermodynamic Properties of Chitosan Constituents by DFT Method, *Int. J. Mater. Sci. Appl.* 3 (2014) 121, doi:10.11648/j.ijmsa.20140304.11.
- [21] M. Emmanuel, A. Pogrebnoi, T. Pogrebnya, Theoretical study of the interaction between chitosan constituents (glucosamine and Acetylglucosamine dimers) and Na⁺ ions, *OALib* 2 (2015) 1–14, <https://doi.org/10.4236/oalib.1101978>.
- [22] X. Gao, W. Liu, H. Liu, S. He, M. Tang, C. Zhu, Reaction mechanism of chitosan/acrylamides dimer: a DFT study, *J. Phys. Org. Chem.* 31 (2018) 1–8, <https://doi.org/10.1002/poc.3775>.
- [23] B.C. Deka, P.K. Bhattacharyya, Understanding chitosan as a gene carrier: a DFT study, *Comput. Theor. Chem.* 1051 (2015) 35–41, <https://doi.org/10.1016/j.comptc.2014.10.023>.
- [24] B.C. Deka, P.K. Bhattacharyya, Response of chitosan-nucleobase interaction toward external perturbations: a computational study, *Comput. Theor. Chem.* 1078 (2016) 72–80, <https://doi.org/10.1016/j.comptc.2015.12.016>.
- [25] B.C. Deka, S.K. Purkayastha, P.K. Bhattacharyya, Formation of thiophene sandwiches through cation- π interaction: a DFT study, *Comput. Theor. Chem.* 1095 (2016) 83–92, <https://doi.org/10.1016/j.comptc.2016.09.018>.
- [26] C. Rajesh, C. Majumder, H. Mizuseki, Y. Kawazoe, A theoretical study on the interaction of aromatic amino acids with graphene and single walled carbon nanotube, *J. Chem. Phys.* 130 (2009), doi:<https://doi.org/10.1063/1.3079096>.
- [27] J. Rezáč, P. Hobza, Benchmark calculations of interaction energies in noncovalent complexes and their applications, *Chem. Rev.* 116 (2016) 5038–5071, <https://doi.org/10.1021/acs.chemrev.5b00526>.
- [28] B.C. Deka, P.K. Bhattacharyya, Reactivity of chitosan derivatives and their interaction with guanine: a computational study, *J. Chem. Sci.* 128 (2016) 589–598, <https://doi.org/10.1007/s12039-016-1064-6>.
- [29] B. Hassan, K. Muraleedharan, V.M. Abdul Mujeeb, Density functional theory studies of Pb(II) interaction with chitosan and its derivatives, *Int. J. Biol. Macromol.* 74 (2015) 483–488, <https://doi.org/10.1016/j.jbiomac.2015.01.006>.
- [30] S. Rahmawati, C.L. Radiman, M.A. Martoprawiro, Density functional theory (DFT) and natural bond orbital (NBO) analysis of intermolecular hydrogen bond interaction in "Phosphorylated nata de coco - water," *Indones. J. Chem.* 18 (2018) 173–178, doi:10.22146/ijc.25170.
- [31] S. Rahmawati, C.L. Radiman, M.A. Martoprawiro, Ab Initio study of proton transfer and hydration on phosphorylated nata de coco, *Indones. J. Chem.* 17 (2017) 523–530, doi:10.22146/ijc.24895.
- [32] F. Foster, J. P. Weinhold, Natural hybrid orbitals, *J. 102*, 7211–7218, *Am. Chem. Soc.* 102 (1980) (1980) 7211–7218.
- [33] A.E. Reed, F. Weinhold, Natural localized molecular orbitals, *J. Chem. Phys.* 83 (1985) 10–1740, <https://doi.org/10.1063/1.449360>.
- [34] A.E. Reed, L.A. Curtiss, F. Weinhold, Intermolecular interactions from a Natural bond orbital, donor-acceptor viewpoint, *Chem. Rev.* 88 (1988) 899–926, <https://doi.org/10.1021/cr00088a005>.
- [35] J. Chocholoušová, V. Špírk, P. Hobza, First local minimum of the formic acid dimer exhibits simultaneously red-shifted O-H...O and improper blue-shifted C-H...O hydrogen bonds, *Phys. Chem. Chem. Phys.* 6 (2004) 37–41, <https://doi.org/10.1039/b314148a>.
- [36] C.K. Sinha, M. Benport, Handbook of pediatric surgery, *Handb. Pediatr. Surg.* XXII (2010) 1–492, https://doi.org/10.1007/978-1-84882-132-3_1.
- [37] S.F. Yannacone, D. Sethio, E. Kraka, Quantitative assessment of intramolecular hydrogen bonds in neutral histidine, *Theor. Chem. Acc.* 139 (2020), doi:<https://doi.org/10.1007/s00214-020-02631-x>.
- [38] J. Klein, H. Khartabil, J.C. Boisson, J. Contreras-García, J.P. Piquemal, E. Hénon, New way for probing bond strength, *J. Phys. Chem. A* 124 (2020) 1850–1860, <https://doi.org/10.1021/acs.jpca.9b09845>.
- [39] G.A. Zhurko, Chemcraft - Graphical Program for Visualization of Quantum Chemistry Computations, <https://www.chemcraftprog.com> 2018. (Accessed 13 March 2019).
- [40] M. Valiev, E.J. Bylaska, N. Govind, K. Kowalski, T.P. Straatsma, H.J.J. Van Dam, D. Wang, J. Nieplocha, E. Apra, T.L. Windus, W.A. De Jong, NWChem: a comprehensive and scalable open-source solution for large scale molecular simulations, *Comput. Phys. Commun.* 181 (2010) 1477–1489, <https://doi.org/10.1016/j.cpc.2010.04.018>.
- [41] P. Singla, M. Riyaz, S. Singhal, N. Goel, Theoretical study of adsorption of amino acids on graphene and BN sheet in gas and aqueous phase with empirical DFT dispersion correction, *Phys. Chem. Chem. Phys.* 18 (2016) 5597–5604, <https://doi.org/10.1039/c5cp07078c>.
- [42] R. Terreux, M. Domard, C. Viton, A. Domard, Interactions study between the copper II ion and constitutive elements of chitosan structure by DFT calculation, *Biomacromolecules* 7 (2006) 31–37, <https://doi.org/10.1021/bm0504126>.
- [43] P. Sikorski, F. Mo, G. Skjåk-Bræk, B.T. Stokke, Evidence for egg-box-compatible interactions in calcium - alginate gels from fiber x-ray diffraction, *Biomacromolecules* 8 (2007) 2098–2103, <https://doi.org/10.1021/bm071503>.
- [44] W. Plazinski, Molecular analysis of calcium binding by polyguluronate chains. Revisiting the egg-box model, *J. Comput. Chem.* 32 (2011) 2988–2995, <https://doi.org/10.1002/jcc.21880>.
- [45] P. Aguilhon, V. Markova, M. Robitzer, F. Quignard, T. Mineva, Structure of alginate gels: interaction of diuronate units with divalent cations from density functional calculations, *Biomacromolecules* 13 (2012) 1899–1907, <https://doi.org/10.1021/bm300420z>.
- [46] W. Plazinski, Conformational properties of acidic oligo- and disaccharides and their ability to bind calcium: a molecular modeling study, *Carbohydr. Res.* 357 (2012) 111–117, <https://doi.org/10.1016/j.carres.2012.04.021>.
- [47] F. Akman, Prediction of chemical reactivity of cellulose and chitosan based on density functional theory, *Cellul. Chem. Technol.* 51 (2017) 253–262.
- [48] P. Emsley, A.T. Brunger, L. Lütke, Tools to assist determination and validation, 1273 (2015) 229–240, <https://doi.org/10.1007/978-1-4939-2343-4>.
- [49] T.A. Sergeyeva, L.A. Gorbach, E.V. Piletska, S.A. Piletsky, O.O. Brovko, L.A. Honcharova, O.D. Lutsyk, L.M. Sergeeva, O.A. Zinchenko, A.V. El'skaya, Colorimetric test-systems for creatinine detection based on composite molecularly imprinted polymer membranes, *Anal. Chim. Acta* 770 (2013) 161–168, <https://doi.org/10.1016/j.aca.2013.01.048>.
- [50] Y.C. Cheng, C.C. Fu, Y.S. Hsiao, C.C. Chien, R.S. Juang, Clearance of low molecular-weight uremic toxins p-cresol, creatinine, and urea from simulated serum by adsorption, *J. Mol. Liq.* 252 (2018) 203–210, <https://doi.org/10.1016/j.molliq.2017.12.084>.
- [51] M. Reth, Matching cellular dimensions with molecular sizes, *Nat. Publ. Gr.* 14 (2013) 765–767, <https://doi.org/10.1038/ni.2621>.
- [52] R. Saber, S. Sarkar, P. Gill, B. Nazari, F. Faridani, High resolution imaging of IgG and IgM molecules by atomic force tunneling microscopy in air condition, *Sci. Iran.* 18 (2011) 1643–1646, <https://doi.org/10.1016/j.scient.2011.11.028>.
- [53] Y. Roy, D.M. Warsinger, J.H. Lienhard, Effect of temperature on ion transport in nanofiltration membranes: diffusion, convection and electromigration, *Desalination* 420 (2017) 241–257, <https://doi.org/10.1016/j.desal.2017.07.020>.
- [54] B. Su, S. Sun, C. Zhao, Polyethersulfone Hollow Fiber Membranes for Hemodialysis, *Prog. Hemodial. - From Emergent Biotechnol. to Clin. Pract.* 2011, <https://doi.org/10.5772/22857>.
- [55] J. Konieczkowska, H. Janeczka, J.G. Malecki, E. Schab-Balcerzak, The comprehensive approach towards study of (azo)polymers fragility parameter: effect of architecture, intra- and intermolecular interactions and backbone conformation, *Eur. Polym. J.* 109 (2018) 489–498, <https://doi.org/10.1016/j.eurpolymj.2018.10.026>.
- [56] P.K. Mondal, V.R. Hathwar, D. Chopra, Characterization of electronic features of intermolecular interactions involving organic fluorine: inputs from in situ cryocrystallization studies on -F and -CF₃ substituted anilines, *J. Fluor. Chem.* 211 (2018) 37–51, <https://doi.org/10.1016/j.jfluchem.2018.03.016>.
- [57] S. Meng, W. Fan, X. Li, Y. Liu, D. Liang, X. Liu, Intermolecular interaction of polysaccharides in membrane fouling during microfiltration, *Water Res.* 143 (2018) 38–46, <https://doi.org/10.1016/j.watres.2018.06.027>.
- [58] E. Rieloff, M.D. Tully, M. Skepö, Assessing the intricate balance of intermolecular interactions upon self-Association of Intrinsically Disordered Proteins, *J. Mol. Biol.* 431 (2019) 511–523, <https://doi.org/10.1016/j.jmb.2018.11.027>.
- [59] F. Sharipov, Influence of quantum intermolecular interaction on internal flows of rarefied gases, *Vacuum* 156 (2018) 146–153, <https://doi.org/10.1016/j.vacuum.2018.07.022>.
- [60] G.A. Dilabio, E.R. Johnson, A. Otero-De-La-Roza, Performance of conventional and dispersion-corrected density-functional theory methods for hydrogen bonding interaction energies, *Phys. Chem. Chem. Phys.* 15 (2013) 12821–12828, <https://doi.org/10.1039/c3cp51559a>.
- [61] B. Saffari, D. Hudiyantri, M.D. Lakstoriini, N.A. Sasongko, P. Siahaan, Intermolecular hydrogen bond interactions in N-methylchitosan and n H₂O: DFT and NBO studies, *AIP Conf. Proc.* 2237 (2020), doi:<https://doi.org/10.1063/50005287>.
- [62] R. Pratiwi, S. Ibrahim, D.H. Tjahjono, Reactivity and stability of Metalloporphyrin complex formation: DFT and experimental study, *Molecules* 25 (2020) 1–8, <https://doi.org/10.3390/molecules25184221>.

- [75] K. Chandrasekaran, R. Thilak Kumar, Structural, spectral, thermodynamical, NLO, HOMO, LUMO and NBO analysis of 5-fluconazole, *Spectrochim. Acta A Mol. Biomol. Spectrosc.* 150 (2015) 974–991, <https://doi.org/10.1016/j.saa.2015.06.018>.
- [76] T. Suzuki, Y. Ishigaki, K. Sugawara, Y. Umezawa, R. Katoono, A. Shimoyama, Y. Manabe, K. Fukase, T. Fukushima, Narrower HOMO–LUMO gap attained by conformational switching through peripheral polyarylation in 1,4-bis(4-phenyl-1H-tetraaza-9,10-anthraquinodimethanes), *Tetrahedron*. 74 (2018) 2239–2244, <https://doi.org/10.1016/j.tet.2018.03.041>.
- [77] M. Bercea, L.M. Gradinaru, M. Mandru, D.L. Tigau, C. Ciobanu, Intermolecular interactions and self-assembling of polyurethane with poly(vinyl alcohol) in aqueous solutions, *J. Mol. Liq.* 274 (2019) 562–567, <https://doi.org/10.1016/j.molliq.2018.11.018>.
- [78] H. Safia, L. Ismahan, G. Abdelkrim, C. Mouna, N. Leila, M. Fatiha, Density functional theories study of the interactions between host β -Cyclodextrin and guest 8-Anilino-naphthalene-1-sulfonate: molecular structure, HOMO, LUMO, NBO, QTAIM and NMR analyses, *J. Mol. Liq.* 280 (2019) 218–229, <https://doi.org/10.1016/j.molliq.2019.01.019>.
- [79] P. Shafieyoon, E. Mehdipour, Y.S. Mary, Synthesis, characterization and biological investigation of glycine-based sulfonamide derivative and its complex: vibration assignment, HOMO – LUMO analysis, MEP and molecular docking, *J. Mol. Struct.* 1181 (2019) 244–252, <https://doi.org/10.1016/j.molstruc.2018.12.067>.
- [80] S. Ghosh, P. Chopra, S. Wategaonkar, C–H...S interaction exhibits all the characteristics of conventional hydrogen bonds, *Phys. Chem. Chem. Phys.* 22 (2020) 17482–17493, <https://doi.org/10.1039/d0cp01508c>.
- [81] Thomas Steiner, The Hydrogen Bond in the Solid State, *Angew. Chemie - Int. Ed. Chem.* (2002) 48–76, <https://doi.org/10.1109/CDC2015.7402694>.
- [82] P. Kolandaivel, V. Nirmala, Study of proper and improper hydrogen bonding using Bader's atoms in molecules (AIM) theory and NBO analysis, *J. Mol. Struct.* 694 (2004) 33–38, <https://doi.org/10.1016/j.molstruc.2004.01.030>.
- [83] M. Rezaei-Sameti, P. Zarei, NBO, AIM, HOMO–LUMO and thermodynamic investigation of the nitrate ion adsorption on the surface of pristine, Al and Ga doped BNNTs: a DFT study, *Adsorption*. 24 (2018) 757–767, <https://doi.org/10.1007/s10450-018-9977-7>.
- [84] T. Lu, F. Chen, Multiwfn: a multifunctional wavefunction analyzer, *J. Comput. Chem.* 33 (2012) 580–592, <https://doi.org/10.1002/jcc.22885>.

The validation of molecular interaction among dimer chitosan with urea and creatinine using density functional theory: In application for hemodialysis membrane

ORIGINALITY REPORT

8%

SIMILARITY INDEX

5%

INTERNET SOURCES

5%

PUBLICATIONS

2%

STUDENT PAPERS

PRIMARY SOURCES

1

onlinelibrary.wiley.com

Internet Source

<1 %

2

Michal Malček, M. Natalia D.S. Cordeiro. "A DFT and QTAIM study of the adsorption of organic molecules over the copper-doped coronene and circumcoronene", Physica E: Low-dimensional Systems and Nanostructures, 2018

Publication

<1 %

3

repositorio.ipen.br

Internet Source

<1 %

4

spotidoc.com

Internet Source

<1 %

5

Sheetal B. Marganakop, Ravindra R. Kamble, Madivalagouda S. Sannaikar, Praveen K. Bayannavar et al. "SCXRD, DFT and molecular docking based structural analyses towards novel 3-piperazin-1-yl-benzo[d]isothiazole and 3-piperidin-4-yl-benzo[d]isoxazoles appended

<1 %

to quinoline as pharmacological agents",
Journal of Molecular Structure, 2022

Publication

6	link.springer.com Internet Source	<1 %
7	vtechworks.lib.vt.edu Internet Source	<1 %
8	sro.sussex.ac.uk Internet Source	<1 %
9	Iryna Khmara, Oliver Strbak, Vlasta Zavisova, Martina Koneracka et al. "Chitosan-stabilized iron oxide nanoparticles for magnetic resonance imaging", Journal of Magnetism and Magnetic Materials, 2018 Publication	<1 %
10	coek.info Internet Source	<1 %
11	home.iitk.ac.in Internet Source	<1 %
12	Masoumeh Bavadi, Khodabakhsh Niknam, Omolbanin Shahraki. "Novel pyrrole derivatives bearing sulfonamide groups: Synthesis in vitro cytotoxicity evaluation, molecular docking and DFT study", Journal of Molecular Structure, 2017 Publication	<1 %

14

Rahul P. Dubey, Urmila H. Patel.
"Crystallography Study, Hirshfeld Surface Analysis and DFT Studies of Cadmium Complex of the Triple Sulfa Drug Constituent Sulfadiazine with Secondary Ligand β -Picoline", Journal of Chemical Crystallography, 2019

Publication

<1 %

15

P. Rajesh, P. Kandan, S. Sathish, A. Manikandan, S. Gunasekaran, T. Gnanasambandan, S. Bala Abirami.
"Vibrational spectroscopic, UV-Vis, molecular structure and NBO analysis of Rabeprazole", Journal of Molecular Structure, 2017

Publication

<1 %

16

Shun-ichi Kawahara, Tadafumi Uchimaru, Kazunari Taira. "Electron correlation and basis set effects on strong hydrogen bond behavior: a case study of the hydrogen difluoride anion", Chemical Physics, 2001

Publication

<1 %

17

Garro, J.C.. "Theoretical study of a hydration mechanism in an enaminone pro-drug prototype", Journal of Molecular Structure: THEOCHEM, 200312

Publication

<1 %

18

donglin.nju.edu.cn

Internet Source

<1 %

19

Aparicio, Santiago, and Rafael Alcalde.

"Insights into the Ethyl Lactate + Water Mixed Solvent", The Journal of Physical Chemistry B, 2009.

Publication

<1 %

20

G. Mahmoudzadeh, R. Ghiasi, H. Pasdar.

"Computational Investigation of the Pseudo Jahn–Teller Effect on the Structure and Chemical Properties of Perhaloethene Anions", Journal of Structural Chemistry, 2019

Publication

<1 %

21

Aliakbar Tehrani, Zahra, Zahra Jamshidi, Marjan Jebeli Javan, and Alireza Fattahi.

"Interactions of Glutathione Tripeptide with Gold Cluster: Influence of Intramolecular Hydrogen Bond on Complexation Behavior", The Journal of Physical Chemistry A, 2012.

Publication

<1 %

22

Xiangjun Meng. "Theoretical Studies on the Proton Transfer through Water Bridges in Hydrated Glycine Cluster", Communications in Computer and Information Science, 2010

Publication

<1 %

23

www.authorea.com

Internet Source

<1 %

24	Ruby Srivastava. "Physicochemical, antioxidant properties of carotenoids and its optoelectronic and interaction studies with chlorophyll pigments", Scientific Reports, 2021 Publication	<1 %
25	Xianglei Kong. "Serine-phosphoric acid cluster ions studied by electrospray ionization and tandem mass spectrometry", Journal of Mass Spectrometry, 06/2011 Publication	<1 %
26	123userdocs.s3-website-eu-west-1.amazonaws.com Internet Source	<1 %
27	Www.duo.uio.no Internet Source	<1 %
28	doc.rero.ch Internet Source	<1 %
29	farfar.pharmacy.bg.ac.rs Internet Source	<1 %
30	motus.org Internet Source	<1 %
31	Kwon, Y.. "Theoretical studies on o-aminofuranaldehyde and o-aminofuranthioaldehyde in reaction field: C-C rotational barriers and intramolecular	<1 %

hydrogen bonding", Journal of Molecular
Structure: THEOCHEM, 20000107

Publication

32

Markku R. Sundberg, Rolf Uggla, Tarja
Laitalainen, Jan Bergman. " Influence of
secondary bonding on the intradimer distance
of trichloro(ethane-1,2-diolato-O,O')tellurate()
", J. Chem. Soc., Dalton Trans., 1994

Publication

<1 %

33

china.iopscience.iop.org

Internet Source

<1 %

34

dais.sanu.ac.rs

Internet Source

<1 %

35

ijasret.com

Internet Source

<1 %

36

repo.lib.tokushima-u.ac.jp

Internet Source

<1 %

37

researchnow.flinders.edu.au

Internet Source

<1 %

38

science.lpnu.ua

Internet Source

<1 %

39

www.hevs.ch

Internet Source

<1 %

40

Farin Windy Artanti, Wega Trisunaryanti,
Marthinus Pongsendana, Triyono, Iip Izul
Falah, Muhammad Fajar Marsuki. "CATALYTIC

<1 %

ACTIVITY TEST OF NiMo AND MoNi
IMPREGNATED ON MESOPOROUS CARBON
FROM BOVINE BONE GELATIN FOR
HYDROCRACKING OF LUBRICANT WASTE",
Rasayan Journal of Chemistry, 2018

Publication

41

Huang, H.. "A screened hybrid density functional study on energetic complexes: Cobalt, nickel and copper carbohydrazide perchlorates", Journal of Hazardous Materials, 20100715

Publication

42

Jingwen Chen, Liansheng Wang. "Acute toxicity of alkyl (1 - phenylsulfonyl) cycloalkane - carboxylates to photobacterium phosphoreum and quantitative structure - activity relationship study based on the AM1 Hamiltonian", Toxicological & Environmental Chemistry, 1996

Publication

43

Urratul Aqyuni, Sukmawati Nur Endah, Priyo Sidik Sasongko, Retno Kusumaningrum, Khadijah, Rismiyati, Hanif Rasyidi. "Waste Image Segmentation Using Convolutional Neural Network Encoder-Decoder with SegNet Architecture", 2020 4th International Conference on Informatics and Computational Sciences (ICICoS), 2020

Publication

<1 %

<1 %

<1 %

44	backend.orbit.dtu.dk Internet Source	<1 %
45	journals.ums.ac.id Internet Source	<1 %
46	m.scirp.org Internet Source	<1 %
47	pubs.rsc.org Internet Source	<1 %
48	researchexperts.utmb.edu Internet Source	<1 %
49	rupress.org Internet Source	<1 %
50	www.iejme.com Internet Source	<1 %
51	Alberto Ruiz, Hiram Pérez, Cercis Morera-Boado, Luis Almagro et al. "Unusual hydrogen bond patterns contributing to supramolecular assembly: conformational study, Hirshfeld surface analysis and density functional calculations of a new steroid derivative", CrystEngComm, 2014 Publication	<1 %
52	Magdalena Małecka, Swastik Mondal, Sander van Smaalen, Carsten Paulmann. " Charge density distribution of 3-(1-	<1 %

aminoethylidene)-2-methoxy-2-oxo-2,3-dihydro-2λ⁻-benzo[] [1,2]oxaphosphinin-4-one", Acta Crystallographica Section B Structural Science, Crystal Engineering and Materials, 2013

Publication

53

Zhi-Xiang Wang, Yong Duan. "Solvation effects on alanine dipeptide: A MP2/cc-pVTZ//MP2/6-31G** study of (,) energy maps and conformers in the gas phase, ether, and water", Journal of Computational Chemistry, 2004

Publication

54

Aymard Didier Tamafo Fouegue, Julius Numbonui Ghogomu, Désiré Bikélé Mama, Nyiang Kennet Nkungli, Elie Younang. "Structural and Antioxidant Properties of Compounds Obtained from Fe Chelation by Juglone and Two of Its Derivatives: DFT, QTAIM, and NBO Studies ", Bioinorganic Chemistry and Applications, 2016

Publication

55

Chengyu Wu, Pan Tao, Jian Li, Yanqing Gao, Shibin Shang, Zhanqian Song. "Antifungal application of pine derived products for sustainable forest resource exploitation", Industrial Crops and Products, 2020

Publication

<1 %

<1 %

<1 %

Exclude quotes Off

Exclude matches Off

Exclude bibliography Off

The validation of molecular interaction among dimer chitosan with urea and creatinine using density functional theory: In application for hemodialysis membrane

GRADEMARK REPORT

FINAL GRADE

/0

GENERAL COMMENTS

Instructor

PAGE 1

PAGE 2

PAGE 3

PAGE 4

PAGE 5

PAGE 6

PAGE 7

PAGE 8

PAGE 9

PAGE 10

PAGE 11